

Communication

Heterogeneous Solid-State Plasticity of a Multi-Functional Metallo-Supramolecular Shape-Memory Polymer towards Arbitrary Shape Programming

Guancong Chen ^{1,2}  and Di Chen ^{1,2,*} ¹ Ningbo Research Institute of Zhejiang University, Ningbo 315100, China; cc_chen@zju.edu.cn² State Key Laboratory of Chemical Engineering, College of Chemical and Biological Engineering, Zhejiang University, Hangzhou 310027, China

* Correspondence: di_chen@zju.edu.cn

Abstract: Shape-memory polymers (SMPs) exhibit notable shape-shifting behaviors under environmental stimulations. In a specific shape-memory cycle, the material can be temporarily fixed at diverse geometries while recovering to the same permanent shape driven by the elastic network, which somewhat limits the versatility of SMPs. Via dynamic metallo-supramolecular interactions, herein, we report a multi-functional shape-memory polymer with tunable permanent shapes. The network is constructed by the metallic coordination of a four-armed polycaprolactone with a melting temperature of 54 °C. Owing to the thermo-induced stress relaxation through the bond exchange, the SMPs can be repeatedly programmed into different geometries in their solid state and show the self-welding feature. Via further welding of films crosslinked by different ions, it will present heterogeneous solid-state plasticity, and a more sophisticated shape can be created after the uniform thermal treatment. With elasticity and plasticity in the same network, the SMPs will display programmable shape-shifting behaviors. Additionally, the used material can be recast into a new film which retains the thermo-induced plasticity. Overall, we establish a novel strategy to manipulate the permanent shapes of SMPs through solid-state plasticity and develop a multi-functional shape-shifting material that has many practical applications.

Keywords: shape-memory polymers; metallo-supramolecular interactions; shape programming; self-welding; reprocessing



Citation: Chen, G.; Chen, D. Heterogeneous Solid-State Plasticity of a Multi-Functional Metallo-Supramolecular Shape-Memory Polymer towards Arbitrary Shape Programming. *Polymers* **2022**, *14*, 1598. <https://doi.org/10.3390/polym14081598>

Academic Editor: Andrea Ehrmann

Received: 18 March 2022

Accepted: 11 April 2022

Published: 14 April 2022

Publisher's Note: MDPI stays neutral with regard to jurisdictional claims in published maps and institutional affiliations.



Copyright: © 2022 by the authors. Licensee MDPI, Basel, Switzerland. This article is an open access article distributed under the terms and conditions of the Creative Commons Attribution (CC BY) license (<https://creativecommons.org/licenses/by/4.0/>).

1. Introduction

Shape shifting is crucial for the survival of creatures such as the mimosa or Venus Flytrap during environmental changes [1]. Inspired by such biological intelligence, the past years have witnessed tremendous developments in synthetic shape-shifting materials, which now play essential roles in diverse fields, including aerospace [2–4], biomedical devices [5,6] and soft electronics [7,8]. Among them, shape-memory polymers (SMPs) show unique shape-changing behaviors from temporary shapes to permanent shapes, triggered by environmental stimulations, such as heat, light or magnetic fields [9–11]. Despite significant improvements in developing triple [12] and multiple shape-memory effects [13], which can achieve programming of two or more temporary shapes for the polymer, all will generally recover to the same permanent shape initially defined by the mold. Post switching the original shapes of SMPs can further promote the versatility of shape-shifting behaviors and innovate much more practical applications. However, owing to elastic networks, the manipulation of the permanent shape is quite challenging.

Dynamic polymer networks show special stress relaxation behaviors through bond exchange stimulated generally by heat or light, which endow the elastic polymers with solid-state plasticity [14–16]. Such unique features have been applied to the materials towards self-healing [17–19], reprocessing [20,21] and micro-manufacturing [22–24]. Via

introducing dynamic bonds, shape-memory networks can be post fabricated into different shapes and permanently fixed after stress relaxation. In this manner, dynamic disulfide SMP has been developed, and it exhibited UV-induced shape-fixing properties [25]. Forgoing the capability of the light permeation, thermo-responsive polycaprolactone and polyurethane shape-memory networks are also established, respectively, and show more sophisticated shape-shifting behaviors through origami and kirigami [26,27].

Furthermore, dynamic metal–ligand interactions are also applied to the SMPs. The high bonding energy ensures stability at room temperature, and it will present dynamic features after triggering by heat [28–30]. The carboxylic and amino groups are usually used to construct the metallo-supramolecular networks [31,32]. Recently, the polymer contained in the pyridine group has been developed and crosslinked by Zn^{2+} ions. The obtained film shows light-induced welding through photo-thermal conversions [33]. Furthermore, metallo-SMPs are also formed and show different shape-shifting behaviors together with self-welding features [34]. Under these circumstances, the permanent shapes can be manipulated by the metal–ligand bond exchange. In addition, stress relaxation kinetics can be easily adjusted by simply replacing the metal ions compared with conventional dynamic covalent bonds [35]. By controlling the diffusion of metal ions in a shape-memory network, the gradient solid-state plasticity has been achieved, and this led to a distinctive shape-shifting behavior [36]. However, the types of permanent shapes are still limited to simple geometries, including folding and twisting shapes. Although the gradient solid-state plasticity can extend the capability of shape manipulations, it has low efficiency and is restricted by ion diffusion kinetics. Therefore, a more adaptive strategy to arbitrarily program the permanent shapes and acquire different shape-shifting behaviors is still required. Here, we integrate the merits of physical metal–ligand interactions (e.g., self-welding, recasting) to reconstruct the permanent shapes of SMPs and establish the heterogeneous solid-state plasticity by welding different ion-doped materials, which can acquire more complex permanent shapes forgoing the ion diffusion. Combining the plasticity and elasticity, the SMPs will show distinct shape-shifting behaviors.

2. Materials and Methods

2.1. Materials

Chloro-2,2':6',2''-Tripyridine was acquired from Aladdin (Shanghai, China). 1,5,7-triazabicyclo [4.4.0] dec-5-ene, 4'-1,3-propanediol, triethylamine, ϵ -caprolactone, and acryloyl chloride were purchased from TCI chemicals (Tianjin, China). Pentaerythritol tetra(3-mercaptopropionate) (PTME) was purchased from Sigma-Aldrich (Shanghai, China). Unless otherwise stated, all chemicals were used as received.

2.2. Methods

2.2.1. Synthesis of 4'-[2-(3-Hydroxyl) Propoxy]-2,2':6',2''-Terpyridine

4'-chloro-2,2':6',2''-terpyridine (2 g), 1,3-propanediol (2.9 g), KOH (2 g), and anhydrous dimethyl sulfoxide (20 mL) were added into a 50 mL flask and reacted under magnetic stirring at 70 °C for 48 h. The produced liquid was poured into deionized water (50 mL) for precipitation. Then, the pH was adjusted to 6.7 by gradually adding hydrochloric solution (10%). The liquid was totally removed by centrifugation, and the remaining solid was vacuum-dried at 70 °C for 48 h. The obtained product was dissolved in methanol at 70 °C and recrystallized at around 0 °C. The crystalline solid was obtained by centrifugation and vacuum-dried at 70 °C for 24 h. In order to acquire pure product, the above recrystallization-based purification process was repeated twice. The used molecule and the acquired product were characterized by 1H -NMR shown in Figure S3.

2.2.2. Synthesis of Polycaprolactone with a Terpyridine end Group (Mn = 5000)

The acquired hydroxyl-terminated terpyridine (1 g), ϵ -caprolactone (17.2 g), and 1,5,7-triazabicyclo [4.4.0] dec-5-ene (0.5 wt%) were added into a 50 mL flask. The reaction was conducted at 120 °C in a nitrogen atmosphere for 10 h. The resulting polymer was

dissolved in toluene and precipitated in cold methanol. The obtained product was vacuum-dried overnight at room temperature. The product was characterized by $^1\text{H-NMR}$ shown in Figure S4.

2.2.3. Synthesis of TPyA

The previously obtained polycaprolactone with a terpyridine end group (20 g), acryloyl chloride (1.08 g), and triethylamine (1.22 g) were co-dissolved in 100 mL toluene at $80\text{ }^\circ\text{C}$ and reacted for 20 h. Following being precipitated in cold ethanol, the obtained solid product was vacuum-dried for 24 h at room temperature. The TPyA was tested by $^1\text{H-NMR}$ shown in Figure S4.

2.2.4. Synthesis of TPy-Ni $^{2+}$ Networks

TPyA (2 g) and PTME (0.0489 g) were dissolved in *N,N*-dimethylformamide (DMF, 2 g). Triethylamine (2 wt%) was added subsequently. The mixture was reacted at $80\text{ }^\circ\text{C}$ for 10 h. The acquired four-armed macro-monomer was characterized by $^1\text{H-NMR}$ and $^{13}\text{C-NMR}$ shown in Figure S1 and Figure S2, respectively. Then $\text{NiCl}_2 \cdot 6\text{H}_2\text{O}$ (0.0474 g) and DMF (2 g) were added into the liquid. The solution was stirred at $140\text{ }^\circ\text{C}$ for 3 min, then transferred into a mold. On removing the solvent at $70\text{ }^\circ\text{C}$ after 10 h, the dynamic film was acquired. By simply changing the mixing metal ions, different films could be obtained.

2.3. Characterization

The shape-memory property was characterized by a dynamic mechanical analyzer (DMA, type: TA Q800). The maximal force was 18 N and the resolution was 0.1 mN. Using stretching mode, the strain and stress could be auto detected. In addition, the temperature could be controlled by a temperature sensor. In order to avoid sliding, the sample was clamped tightly. Differential scanning calorimetry (DSC) measurements were conducted using a TA Q2000 machine under N_2 at a temperature ramping rate of $5\text{ }^\circ\text{C}/\text{min}$. Mechanical tests were performed using a Zwick/Roell tensile machine at a stretching speed of 10 mm/min and the sample geometry was $25\text{ mm} \times 5\text{ mm} \times 0.3\text{ mm}$. The applied force sensor was 1.5 kN, and it utilized physical clamps.

3. Results and Discussion

Here, we prepare a metallo-supramolecular shape-memory network, and establish diverse shape manipulation approaches using self-welding and solid-state plasticity. Specifically, the shape-memory polymer network is formed by the two-step methods shown in Figure 1. The initial four-armed macro-monomer was prepared through a thiolene click reaction of a polycaprolactone acrylate containing terpyridine (TPy) and pentaerythritol tetrakis (3-mercaptopropionate). After mixing with the metal ion solution, it turns to a shape-memory network via the metal–ligand interactions.

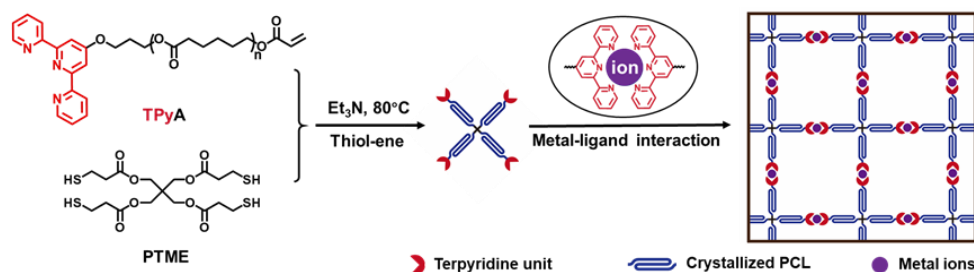


Figure 1. Process of constructing the metallo-supramolecular shape-memory network.

TPy can coordinate with diverse metal ions, and the colors of the obtained films are changed accordingly, as can be seen in Figure 2a. On the contrary, the transition temperatures are all around $54\text{ }^\circ\text{C}$, which was derived from the melting of crystallized

polycaprolactone (PCL) domains (Figure 2b). Since the utilized polycaprolactone is at the same molecular weight, the relative transition temperatures are similar.

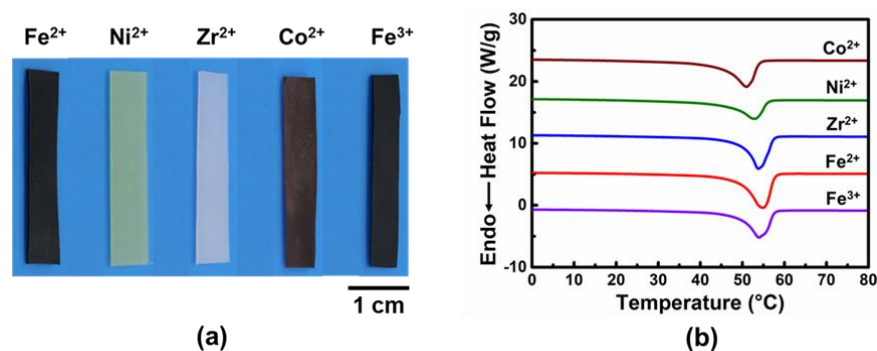


Figure 2. Features of acquired SMPs. (a) Appearance of the films doped with different metal ions. (b) The differential scanning calorimetry curves.

Generally, the phase transition is the key issue for the shape-memory effect. Figure 3a indicates three typical shape-memory cycles of the film doped with Ni^{2+} . Specifically, the Ni^{2+} -doped sample was heated to 65 °C for melting PCL. In the meantime, the sample was stretched under 0.3 MPa stress. After cooling to 0 °C, the sample was fixed at a strain of 38.8%. Following removal of the applied stress, the sample recovered slightly, and the final strain was fixed at 38.6%. Thus, the fixing ratio is 99.5%. When re-heating to 65 °C, the sample recovered to its original state because of the melting of PCL, and the recovery ratio was 93%. The same process was applied to the Co^{2+} doped sample, which showed decent shape-memory behavior with the fixing ratio at 99.6% and a recovery ratio at 98%, as shown in Figure 3b. Figure 3c,d show the testing machine and loading cabin.

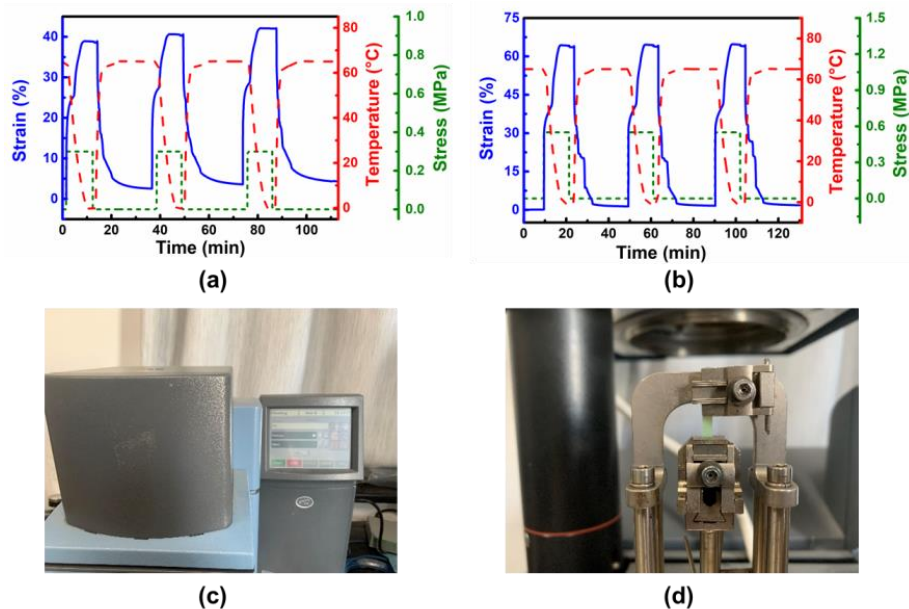


Figure 3. Shape-memory properties of samples doped by Ni^{2+} (a) and Co^{2+} (b). The photos of the DMA machine (c) and the loading cabin (d).

Owing to the dynamic nature of metal–ligand interactions, the SMPs can undergo a thermo-induced bond exchange, which can release internal stress, thus realizing the solid-state plasticity. Meanwhile, the previous stress relaxation kinetics is determined by the utilized metal ions. As seen in Figure 4, at 60 °C, which is close to the melting temperature, samples doped with Fe^{3+} , Fe^{2+} and Zr^{2+} can rapidly relax the stretched networks. Under these circumstances, there is a significant adverse impact on the shape-memory behaviors,

which rely on the elasticity of the networks. On the contrary, the stress relaxation rates of the film containing Co^{2+} are too slow. By comparison, the polymer network doped by Ni^{2+} possesses an acceptable relaxation rate, and exhibits distinctive shape-memory behaviors as clearly shown in Figure 3a above. Therefore, due to the controllable elasticity and plasticity of Ni^{2+} doped films, we generally used them as the model materials for the following demonstrations.

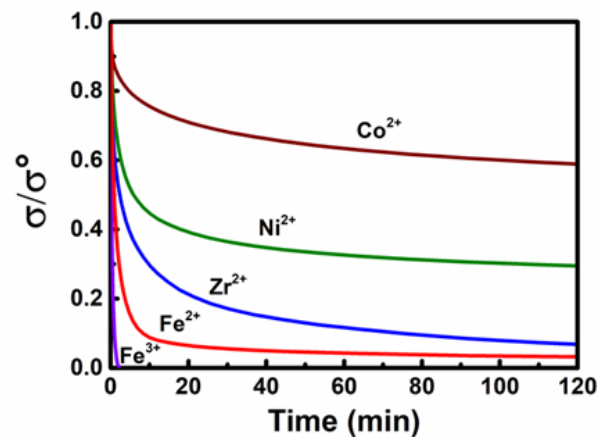


Figure 4. The stress relaxation kinetics of different metal ions doped samples at 60 °C. σ represents the instantaneous stress and σ° represents the initial stress.

Solid-state plasticity is further influenced by temperatures. As shown in Figure 5, the relaxation rates of Ni^{2+} -doped samples accelerated along with the increase in temperature. In addition, the shape retention increased from 30% at 60 °C to 100% at 120 °C. Consequently, we can set the network into an adaptive capability of plasticity by switching temperatures in a specific shape-shifting process.

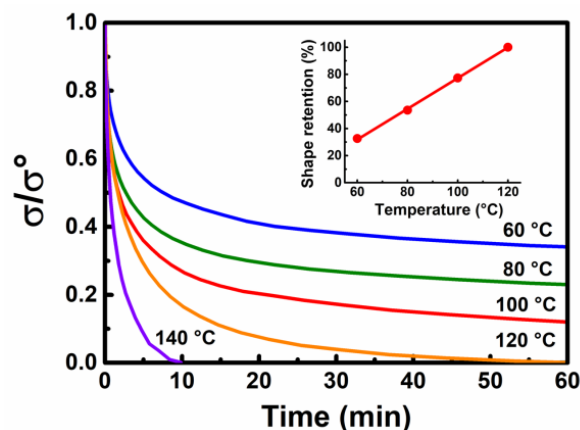


Figure 5. The stress relaxation properties of Ni^{2+} -doped films at different temperatures, and inserts show the shape retention.

Using the up-mentioned solid-state plasticity, we can program the permanent shapes of a shape-memory polymer. Utilizing the Ni^{2+} -doped samples, the 2D film can be folded into different 3D geometries and permanently fixed by heating at 140 °C for 10 min. Using this method, bird- and elephant-shaped SMPs can be obtained (shown in Figure 6).

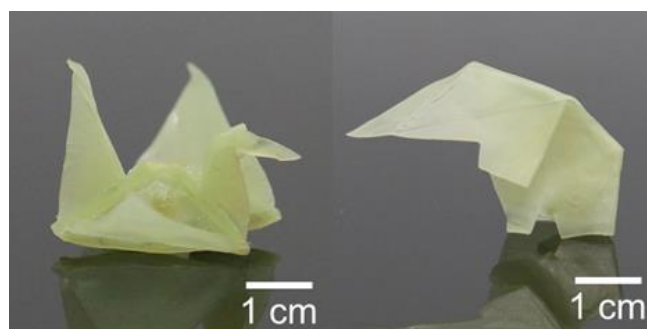


Figure 6. SMPs with permanent shapes of a bird and an elephant, respectively.

With distinctive elasticity and plasticity in our metallo-supramolecular shape-memory networks, they can exhibit unique shape-shifting behaviors in a more programmable way. As seen in Figure 7, a rectangular film (Shape A) is folded and permanently fixed into an airplane shape (Shape B) by heating it at 140 °C for 10 min. When the temperature switches to 65 °C, it turns to its rubbery state because of the melting of the PCL domain and can be opened to a planar film (Shape C), which is temporarily locked by cooling. After re-heating to 65 °C, the planar film will recover to the airplane shape (Shape B) again due to its elasticity. In addition, the polymer with an airplane shape (Shape B) can be reprogrammed into a boat shape (Shape D) via solid-state plasticity under 140 °C and can be temporarily changed to either a curved structure (Shape E) or a planar structure (Shape F) by crystallization of PCL domains, which will all recover to the boat shape over the melting temperature. The above diverse shape-shifting behaviors exactly present the merits of our metallo-supramolecular networks. The shape memory process can be triggered at a relatively low temperature, while the permanent shape can be programmed at a higher temperature. Both can be independently regulated. Theoretically, the number of obtained shape-shifting modes is infinite.

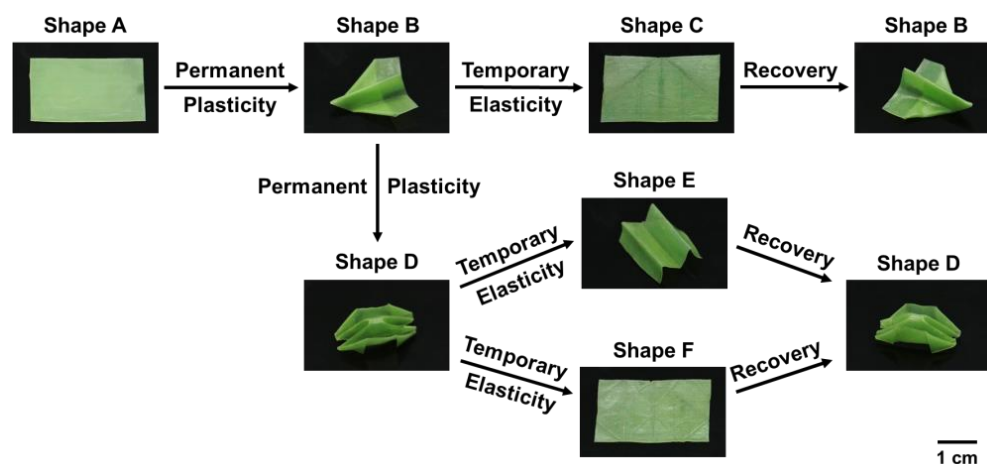


Figure 7. The diverse shape-shifting behaviors via a metallo-supramolecular shape-memory film.

Physical metallo-supramolecular interactions further provide the networks with self-welding properties that can create more complex forms via assembly. As indicated in Figure 8a, the mechanical properties of films before and after welding are very similar, revealing good self-welding capabilities. Thus, as shown in Figure 8b, we programmed the planar films into a windmill shape and a shaft shape, respectively, by solid-state plasticity. The two parts were further assembled into a windmill tower through thermo-induced self-welding. In this way, more sophisticated shapes can be established beyond conventional origami [37].

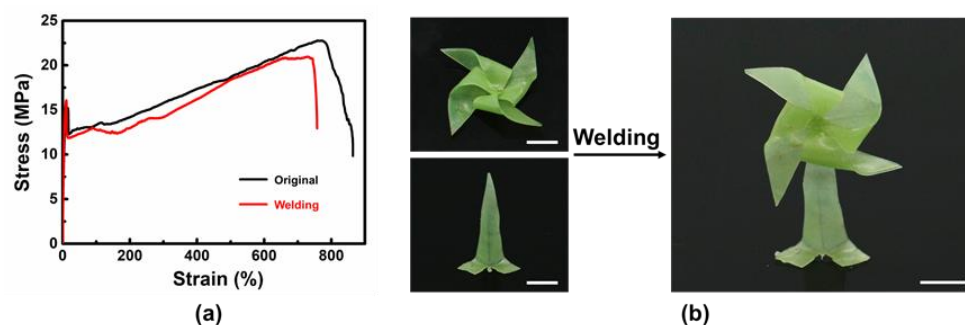


Figure 8. The self-welding of metallo-supramolecular networks. (a) The mechanical properties of an original sample and a welded sample. (b) A windmill tower shape obtained from self-welding of different parts, scale bar: 1 cm.

Utilizing macroscopic welding of blocks with different stress relaxation kinetics, heterogeneous solid-state plasticity, can be realized, which extends the shape-memory behaviors. As shown in Figure 9, a Ni^{2+} -doped film (light green) and a Co^{2+} -doped film (dark brown) were welded and uniformly folded. After heating at $140\text{ }^{\circ}\text{C}$ for 10 min, the bottom Ni^{2+} -doped part was totally relaxed, while the top Co^{2+} -doped part still possessed internal stress. Because of this imbalance, a permanent fan shape was obtained. With subsequent heating and cooling, the film could be temporarily fixed at the planar sheet, which recovered to the fan shape over the melting temperature. Such shape-memory behavior can be repeatedly triggered because of the elasticity. As a result, it establishes the heterogeneous solid-state plasticity by film welding, which no longer needs to control ion diffusion to achieve the spatial manipulation of plasticity [31].

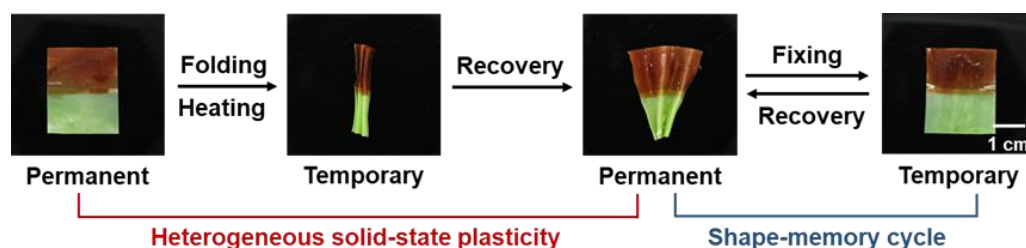


Figure 9. Shape-shifting of a welded film with two different parts.

In addition, a sample with triple blocks is also established in Figure 10. Via the homogeneous thermal treatment at $140\text{ }^{\circ}\text{C}$, two ends were totally fixed, while the central zone was only partially locked; thus, a new permanent shape was constructed. Meanwhile, the sample still maintains the shape-memory property because of the elastic network. The idea of welding film blocks crosslinked by different metal ions can construct complex, permanent shapes of SMPs and absolutely extend the versatility of shape-shifting behaviors.

Finally, the used materials can be dissolved in dimethylformamide at $150\text{ }^{\circ}\text{C}$ and recast into a new film, owing to the dissociation of dynamic metal–ligand bonds during thermo-induced exchange. The process is shown in Figure 11. After recasting, the newly formed film maintains the capability of solid-state plasticity and can be permanently programmed into another shape. Generally, this allows the reuse of material resources.

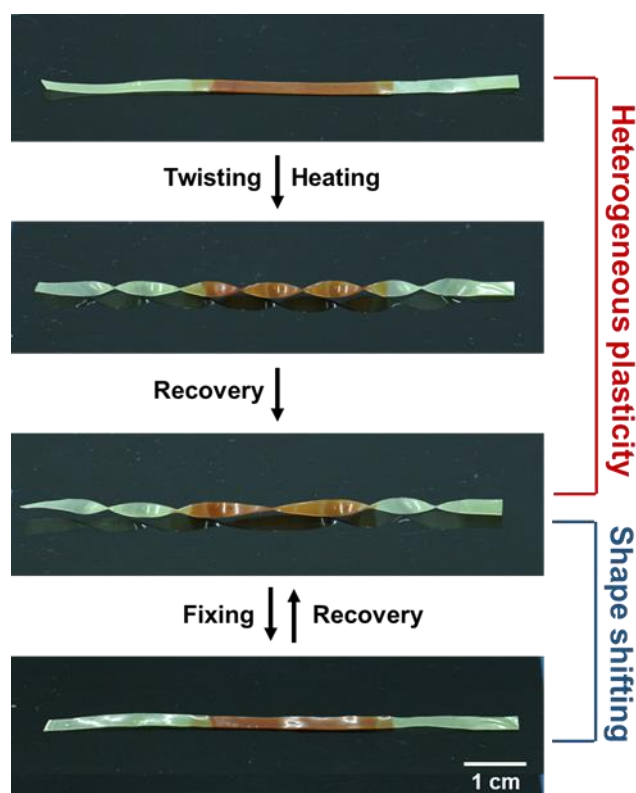


Figure 10. Shape manipulations of a sample with triple blocks.



Figure 11. The recasting and reprogramming of the used sample.

4. Conclusions

In summary, we have prepared a novel metallo-supramolecular shape-memory polymer network crosslinked by metal–ligand bonds. Derived from the thermo-induced bond exchange, the network can be programmed into arbitrary permanent shapes in its solid state, which presents solid-state plasticity. Moreover, with plasticity and elasticity in the same network, it shows distinctive shape-shifting behaviors. With further welding of shape-memory polymer blocks holding different stress relaxation kinetics, a more complex form can be obtained via the heterogeneous solid-state plasticity after the uniform thermal treatment, which distinguishes this research from other currently reported shape programming approaches. Final reprocessing by dissolving and casting improves the capability of shape manipulations and increases the efficiency of resource utilization. By applying the established strategy on adaptive shape manipulations, we envision that our multi-functional dynamic SMPs can be applied to many deployable devices. In addition, the idea of assembling diverse blocks into a new film can achieve the spatial selectivity of different properties (such as modulus, wetting) after uniform thermal treatments.

Supplementary Materials: The following supporting information can be downloaded at: <https://www.mdpi.com/article/10.3390/polym14081598/s1>, Figure S1: The $^1\text{H-NMR}$ spectrum of the four-armed macro-monomer; Figure S2: The $^{13}\text{C-NMR}$ spectrum of the four-armed macro-monomer; Figure S3: The $^1\text{H-NMR}$ spectrum of the Chloro-2,2':6',2''-Tripyridine (left) and hydroxyl terminated TPy (right); Figure S4: The $^1\text{H-NMR}$ spectrum of the polycaprolactone with a terpyridine end group (left) and TPyA (right).

Author Contributions: Methodology, G.C.; Validation, G.C.; Formal Analysis, G.C. and D.C.; Investigation, D.C.; Writing—Original Draft Preparation, D.C.; Review and Editing, G.C. and D.C.; Supervision, D.C. All authors have read and agreed to the published version of the manuscript.

Funding: This research was funded by Start-up funding of Ningbo Research Institute of Zhejiang University (Grant No. 20201203Z0193), the National Science Foundation of China (Grant No. 22105167).

Data Availability Statement: The data presented in this study are available in the article.

Conflicts of Interest: The authors declare no conflict of interest.

References

1. Lee, E.; Yang, S. Bio-inspired responsive polymer pillar arrays. *MRS Commun.* **2015**, *5*, 97–114. [[CrossRef](#)]
2. Zirbel, S.A.; Lang, R.J.; Thomson, M.W.; Sigel, D.A.; Walkemeyer, P.E.; Trease, B.P.; Magleby, S.P.; Howell, L.L. Accommodating thickness in origami-based deployable arrays. *J. Mech. Des.* **2013**, *135*, 111005. [[CrossRef](#)]
3. Aharonia, H.; Xia, Y.; Zhang, X.; Kamienna, R.D.; Yang, S. Universal inverse design of surfaces with thin nematicelastomer sheets. *Proc. Natl. Acad. Sci. USA* **2018**, *115*, 7206–7211. [[CrossRef](#)] [[PubMed](#)]
4. Liu, Y.; Du, H.; Liu, L.; Leng, J. Shape memory polymers and their composites in aerospace applications: A review. *Smart Mater. Struct.* **2014**, *23*, 023001. [[CrossRef](#)]
5. Lendlein, A.; Langer, R. Biodegradable, elastic shape-memory polymers for potential biomedical applications. *Science* **2002**, *5573*, 1673–1676. [[CrossRef](#)] [[PubMed](#)]
6. Ni, C.; Chen, D.; Zhang, Y.; Xie, T.; Zhao, Q. Autonomous shapeshifting hydrogels via temporal programming of photoswitchable dynamic network. *Chem. Mater.* **2021**, *33*, 2046–2053. [[CrossRef](#)]
7. Xu, S.; Yan, Z.; Jang, K.-I.; Huang, W.; Fu, H.; Kim, J.; Wei, Z.; Flavin, M.; McCracken, J.; Wang, R.; et al. Assembly of micro/nanomaterials into complex, three-dimensional architectures by compressive buckling. *Science* **2015**, *347*, 154–159. [[CrossRef](#)]
8. Khan, M.R.; Hayes, G.J.; So, J.-H.; Lazzi, G.; Dickey, M.D. A frequency shifting liquid metal antenna with pressure responsiveness. *Appl. Phys. Lett.* **2011**, *99*, 013501. [[CrossRef](#)]
9. Zhao, Q.; Qi, H.J.; Xie, T. Recent progress in shape memory polymer: New behavior, enabling materials, and mechanistic understanding. *Prog. Polym. Sci.* **2015**, *49–50*, 79–120. [[CrossRef](#)]
10. Lendlein, A.; Behl, M.; Hiebl, B.; Wischke, C. Shape-memory polymers as a technology platform for biomedical applications. *Expert Rev. Med. Devices* **2010**, *7*, 357–379. [[CrossRef](#)]
11. Chen, H.; Wang, L.; Zhou, S. Recent progress in shape memory polymers for biomedical applications. *Chin. J. Polym. Sci.* **2018**, *36*, 905–917. [[CrossRef](#)]
12. Bellin, I.; Kelch, S.; Langer, R.; Lendlein, A. Polymeric triple-shape materials. *Proc. Natl. Acad. Sci. USA* **2006**, *103*, 18043–18047. [[CrossRef](#)] [[PubMed](#)]
13. Xie, T. Tunable polymer multi-shape memory effect. *Nature* **2010**, *464*, 267–270. [[CrossRef](#)] [[PubMed](#)]
14. Zou, W.; Dong, J.; Luo, Y.; Zhao, Q.; Xie, T. Dynamic covalent polymer networks: From old chemistry to modern day innovations. *Adv. Mater.* **2017**, *29*, 1606100. [[CrossRef](#)]
15. Scott, T.F.; Schneider, A.D.; Cook, W.D.; Bowman, C.N. Photoinduced plasticity in cross-linked polymers. *Science* **2005**, *308*, 1615–1617. [[CrossRef](#)]
16. Zheng, N.; Xu, Y.; Zhao, Q.; Xie, T. Dynamic covalent polymer networks: A molecular platform for designing functions beyond chemical recycling and self-healing. *Chem. Rev.* **2021**, *121*, 1716–1745. [[CrossRef](#)]
17. Mozdehi, D.; Ayala, S.; Cromwell, O.R.; Guan, Z. Self-healing multiphase polymers via dynamic metal-ligand interactions. *J. Am. Chem. Soc.* **2014**, *136*, 16128–16131. [[CrossRef](#)]
18. Zeng, Y.; Li, J.; Liu, S.; Yang, B. Rosin-based epoxy vitrimers with dynamic boronic ester bonds. *Polymers* **2021**, *13*, 3386. [[CrossRef](#)]
19. Borre, E.; Stumbe, J.F.; Bellemin-Lapponnaz, S.; Mauro, M. Light-powered self-healable metallocsupramolecular soft actuators. *Angew. Chem. Int. Ed.* **2016**, *55*, 1313–1317. [[CrossRef](#)]
20. Wang, X.; Zhan, S.; Lu, Z.; Li, J.; Yang, X.; Qiao, Y.; Men, Y.; Sun, J. Healable, recyclable, and mechanically tough polyurethane elastomers with exceptional damage tolerance. *Adv. Mater.* **2020**, *32*, 2005759. [[CrossRef](#)]
21. Montarnal, D.; Capelot, M.; Tournilhac, F.; Leibler, L. Silica-like malleable materials from permanent organic networks. *Science* **2011**, *334*, 965–968. [[CrossRef](#)] [[PubMed](#)]
22. Kloxin, C.J.; Scott, T.F.; Park, H.Y.; Bowman, C.N. Mechanophotopatterning on a photoresponsive elastomer. *Adv. Mater.* **2011**, *23*, 1977–1981. [[CrossRef](#)] [[PubMed](#)]
23. Chen, D.; Ni, C.; Xie, L.; Li, Y.; Deng, S.; Zhao, Q.; Xie, T. Homeostatic growth of dynamic covalent polymer network toward ultrafast direct soft lithography. *Sci. Adv.* **2021**, *7*, eabi7360. [[CrossRef](#)] [[PubMed](#)]
24. Fairbanks, B.D.; Singh, S.P.; Bowman, C.N.; Anseth, K.S. Photodegradable, photoadaptable hydrogels via radical-mediated disulfide fragmentation reaction. *Macromolecules* **2011**, *44*, 2444–2450. [[CrossRef](#)] [[PubMed](#)]
25. Michal, B.T.; Jaye, C.A.; Spencer, E.J.; Rowan, S.J. Inherently photohealable and thermal shape-memory polydisulfide networks. *ACS Macro. Lett.* **2013**, *2*, 694–699. [[CrossRef](#)]

26. Zhao, Q.; Zou, W.; Luo, Y.; Xie, T. Shape memory polymer network with thermally distinct elasticity and plasticity. *Sci. Adv.* **2016**, *2*, e1501297. [[CrossRef](#)]
27. Zheng, N.; Fang, Z.; Zou, W.; Zhao, Q.; Xie, T. Thermoset shape-memory polyurethane with intrinsic plasticity enabled by transcarbamoylation. *Angew. Chem. Int. Ed.* **2016**, *128*, 11593–11597. [[CrossRef](#)]
28. Kumpfer, J.R.; Rowan, S.J. Thermo-, photo-, and chemo-responsive shape-memory properties from photo-cross-linked metallo-supramolecular polymers. *J. Am. Chem. Soc.* **2011**, *133*, 12866–12874. [[CrossRef](#)]
29. Whittell, G.R.; Hager, M.D.; Schubert, U.S.; Manners, I. Functional soft materials from metallopolymer and metallosupramolecular polymers. *Nat. Mater.* **2011**, *10*, 176–188. [[CrossRef](#)]
30. Neal, J.A.; Oldenhuis, N.J.; Novitsky, A.L.; Samson, E.M.; Thrift, W.J.; Ragan, R.; Guan, Z. Large continuous mechanical gradient formation via metal-ligand interactions. *Angew. Chem. Int. Ed.* **2017**, *56*, 15575–15579. [[CrossRef](#)]
31. Sun, J.-Y.; Zhao, X.; Illeperuma, W.R.K.; Chaudhuri, O.; Oh, K.H.; Mooney, D.J.; Vlassak, J.J.; Suo, Z. Highly stretchable and tough hydrogels. *Nature* **2012**, *489*, 133–136. [[CrossRef](#)] [[PubMed](#)]
32. Bode, S.; Zedler, L.; Schacher, F.H.; Dietzek, B.; Schmitt, M.; Popp, J.; Hager, M.D.; Schubert, U.S. Self-healing polymer coatings based on crosslinked metallosupramolecular copolymers. *Adv. Mater.* **2013**, *25*, 1634–1638. [[CrossRef](#)] [[PubMed](#)]
33. Burnworth, M.; Tang, L.; Kumpfer, J.R.; Duncan, A.J.; Beyer, F.L.; Fiore, G.L.; Rowan, S.J.; Weder, C. Optically healable supramolecular polymers. *Nature* **2011**, *472*, 334–337. [[CrossRef](#)] [[PubMed](#)]
34. Wang, Z.; Fan, W.; Tong, R.; Lu, X.; Xia, H. Thermal-healable and shape memory metallosupramolecular poly(n-butyl acrylate-co-methyl methacrylate) materials. *RSC Adv.* **2014**, *4*, 25486–25493. [[CrossRef](#)]
35. Mozhdehi, D.; Neal, J.A.; Grindy, S.C.; Cordeau, Y.; Ayala, S.; Holten-Andersen, N.; Guan, Z. Tuning dynamic mechanical response in metallopolymer networks through simultaneous control of structural and temporal properties of the networks. *Macromolecules* **2016**, *49*, 6310–6321. [[CrossRef](#)]
36. Yang, L.; Zhang, G.; Zheng, N.; Zhao, Q.; Xie, T. A Metallosupramolecular shape-memory polymer with gradient thermal plasticity. *Angew. Chem. Int. Ed.* **2017**, *56*, 12599–12602. [[CrossRef](#)] [[PubMed](#)]
37. Manen, T.V.; Janbaz, S.; Amir, A.; Zadpoor, A.A. Programming the shape-shifting of flat soft matter. *Mater. Today* **2018**, *21*, 144–163. [[CrossRef](#)]